

## Osteoblast biocompatibility and inhibition of bacterial adhesion to thermally and chemically treated TiAlV alloy

Greta Tavares-Martínez<sup>a</sup>, Belén Criado<sup>b</sup>, M. Coronada Fernández-Calderón<sup>c,d</sup>, Edgar Onofre-Bustamante<sup>a</sup>, Ciro Pérez-Giraldo<sup>c,d</sup>, Cristina García-Alonso<sup>b,\*</sup>, M<sup>a</sup> Lorenza Escudero<sup>b,\*</sup>

<sup>a</sup> National Polytechnic Institute, Centro de Investigación Ciencia Aplicada y Tecnología Avanzada, Unidad Altamira, Km 14.5 Carretera Tampico-Puerto Industrial, 89600 Altamira, Tamaulipas, México

<sup>b</sup> Spanish National Research Council, National Center for Metallurgical Research (CSIC, CENIM), Department of Surface Engineering, Corrosion and Durability, Avda. Gregorio del Amo 8, 28040 Madrid, Spain

<sup>c</sup> Biomedical Research Centre in Bioengineering, Biomaterials and Nanomedicine Network (CIBER-BBN), Badajoz, Spain

<sup>d</sup> University of Extremadura, Faculty of Medicine and INUBE, Department of Biomedical Sciences, Area of Microbiology, Badajoz, Spain

(\*Corresponding author: [escudero@cenim.csic.es](mailto:escudero@cenim.csic.es))

Submitted: 27 July 2021; Accepted: 8 November 2021; Available On-line: 30 December 2021

**ABSTRACT:** The objective of this work was to study whether thermal and chemical conversion treatments improve the biocompatibility of the TiAlV alloy and reduce bacterial growth. Firstly, TiAlV alloy was modified by thermal treatment at 650 °C for 1 hour. Then, chemical conversion was carried out in a CeCl<sub>3</sub> solution to generate cerium oxide. Modified surfaces were characterized using AFM and SEM-EDX. Osteoblast adhesion and bacteria biofilm formation were measured in vitro with MC3T3-E1 osteoblast cell line and *Staphylococcus epidermidis* ATCC 35983, respectively. Bacterial viability was quantified through content in adenosine triphosphate (ATP) as a measure of metabolic activity. Morphology and proliferation on modified surfaces were analyzed by SEM-EDX. Results revealed that thermally treated TiAlV showed greater osteoblast proliferation viability associated with greater roughness and crystalline structure of rutile. Modified surfaces did not cause bactericidal effect but TiAlV surfaces with ceria showed a decrease in bacterial adhesion i.e. less bacteria proliferation and therefore a decrease in bacterial colonization.

**KEYWORDS:** Nanocerium deposition; Osteoblasts MC3T3-E1; *Staphylococcus epidermidis*; TiAlV; Thermal treatment

Citation/Citar como: Tavares-Martínez, G.; Criado, B.; Fernández-Calderón, M.C.; Onofre-Bustamante, E.; Pérez-Giraldo, C.; García-Alonso, C.; Escudero, M.L. (2021). "Osteoblast biocompatibility and inhibition of bacterial adhesion to thermally and chemically treated TiAlV alloy". *Rev. Metal.* 57(4): e208. <https://doi.org/10.3989/revmetalm.208>

**RESUMEN:** *Biocompatibilidad de osteoblastos e inhibición de adhesión bacteriana a la aleación Ti6Al4V tratada térmica y químicamente.* El objetivo de este trabajo ha sido estudiar si los tratamientos térmicos y de conversión química mejoran la biocompatibilidad de la aleación TiAlV y reducen el crecimiento bacteriano. En primer lugar, se modificó la aleación de TiAlV mediante tratamiento térmico a 650 °C durante 1 hour. Luego, se llevó a

**Copyright:** © 2021 CSIC. This is an open-access article distributed under the terms of the Creative Commons Attribution 4.0 International (CC BY 4.0) License.

cabo la conversión química en una solución de  $\text{CeCl}_3$  para generar óxido de cerio. Las superficies modificadas se caracterizaron utilizando AFM y SEM-EDX. La adhesión de osteoblastos y la formación de biopelículas microbianas se midieron *in vitro* con la línea celular de osteoblastos MC3T3-E1 y *Staphylococcus epidermidis* ATCC 35983, respectivamente. La viabilidad bacteriana se cuantificó a través del contenido en trifosfato de adenosina (ATP) como medida de la actividad metabólica. La morfología y la proliferación en superficies modificadas se analizaron mediante SEM-EDX. Los resultados revelaron que el TiAlV tratado térmicamente mostró una mayor proliferación osteoblástica asociada con una mayor rugosidad y estructura cristalina del rutilo. Las superficies modificadas no causaron efecto bactericida, pero las superficies de TiAlV con ceria mostraron una disminución en la adhesión bacteriana, es decir, menos proliferación bacteriana y por tanto disminución en la colonización bacteriana.

**PALABRAS CLAVE:** Depósito de nanocería; Osteoblastos MC3T3-E1; *Staphylococcus epidermidis*; TiAlV; Tratamiento térmico

**ORCID ID:** Greta Tavarez-Martínez (<https://orcid.org/0000-0002-2625-3052>); Belén Criado (<https://orcid.org/0000-0002-5486-9604>); M. Coronada Fernández-Calderón (<https://orcid.org/0000-0001-8567-6787>); Edgar Onofre-Bustamante (<https://orcid.org/0000-0002-5706-887X>); Ciro Pérez-Giraldo (<https://orcid.org/0000-0002-2358-1982>); Cristina García-Alonso (<https://orcid.org/0000-0003-0275-4626>); M<sup>a</sup> Lorenza Escudero (<https://orcid.org/0000-0002-2181-448X>)

## 1. INTRODUCTION

Material-tissue interface and the long-term success or failure of the integration of an implant in the body are closely correlated with the properties of the implant devices and specifically with their surface properties, such as wettability, texture or chemical composition. The TiAlV alloy has an excellent *in vivo* performance, which makes it the most commonly used prosthetic metallic materials for rods in prostheses for joint and dental implants. However, new research into this alloy, based on the changes in chemical composition, has been carried out with the aim of obtaining alloys with optimal microstructures designed to achieve mechanical properties similar to those of bone and with high corrosion resistance and enhanced biocompatibility promoted by faster integration with bone tissue and minimum bacterial proliferation (Mareci *et al.*, 2009).

The addition of elements in minor contents can determine the surface performance of Ti-based alloys. The vanadium content in this alloy cause toxicity over time, when interacting with biological systems as some studies have reported (Siqueira *et al.*, 2009). So research has been addressed to produce new alloys with a Ti base where the V has been substituted by other elements, such as Fe, which also stabilizes the  $\beta$  phase in the alloy (Simsek and Ozyurek, 2019). Other alloys that have been under investigation using Niobium and Iron instead of Vanadium are, for example, Ti6Al7Nb and Ti5Al2.5Fe ( $\alpha+\beta$ ) phase (Ninomi, 2002; Jackson and Ahmed, 2007). Research of the wear and corrosion behavior of Ti5Al2.5Fe and Ti6Al4V alloys processed by mechanical alloying in a simulated body environment show that although there is an improvement in the wear resistance, both alloys show pitting corrosion in simulated fluids at body temperature (Simsek and Ozyurek, 2019). Alloying elements such as Al, V, and Nb in titanium alloys may be incorporated into the thin oxide film and that probably influences the adsorption of proteins and their accommodation on the surface, modifying the surface-cell interaction (Jenko *et al.*, 2018).

Other surface property, which has an effect on the interaction with proteins is the isoelectric point of the surface which can change depending on the elements that are alloyed (Sittig *et al.*, 1999).

On the other hand, the modification of the surfaces of these alloys are also performed in order to improve their properties of biocompatibility and osseointegration and their resistance to bacterial colonization. It is known that *Staphylococcus species* is responsible for more than 60% of prosthetic infections (Zorn *et al.*, 2011). Bacteria may also be the cause of the orthopedic implant removal following aseptic loosening (Geetha *et al.*, 2009; Raphael *et al.*, 2016). Specifically, *Staphylococcus epidermidis* form biofilms on the prostheses surface, being the principal causes of antibiotic resistance and responsible for the implant replacement (Mareci *et al.*, 2009). So, the success of the implant is based on promoting osseointegration and inhibiting microbial adhesion.

Bearing in mind the importance of this, new surface modification procedures are being developed that do not impair the mechanical properties of the alloys used in biomedical applications (Zorn *et al.*, 2011; Bauer *et al.*, 2013). As regards the TiAlV alloy, the synthesis of nanostructured layers of  $\text{TiO}_2$ , obtained by anodization has been proposed to achieve a better osseointegration, and enhancement of strong, long-lasting bonding between the implant surface and the surrounding bone (Hernández-López *et al.*, 2016; Germán-Salló and Strnad, 2018). A hydrothermal method for producing nanostructures on the TiAlV surface has also been proposed for improving the cellular response (Srivastava *et al.*, 2019). Other surface modifications have been made focused on the technical aspects, such as the grafting of bioactive molecules, with enhanced osseointegration properties (Wu *et al.*, 2014; Yang *et al.*, 2017) or treatments that permit the incorporation of salts or metals to improve osteogenesis and calcification after implantation (Santander *et al.*, 2014; Bral and Mommaerts, 2016).

In the same way, another important development has been driven towards surface modifications to

promote a bactericide effect to prevent the adhesion and proliferation of microorganisms, thus reducing the probability of both short and long term infection. One proposal has been to obtain surfaces covered with lysozyme. The use of lysozyme prevented *Staphylococcus aureus* adhesion, while maintaining high cytocompatibility with the important cell lines (Díaz-Gómez *et al.*, 2018). Also, a proposal has been made studying the combined effect of alumina and zinc on aluminum alloys, where their osteogenic and antibacterial aspects have been studied. As a result, it has been found that the Zn-doped  $\text{Al}_2\text{O}_3$  coating delivers outstanding osteogenesis and antibacterial properties, which makes it a promising candidate for use in bone implants (Weng *et al.*, 2018). Following up this line of research, the TiAlV has been coated with MgCu by arc ion plating in order to improve its bioactivity and in particular its antibacterial properties. The MgCu coating degraded and gradually disappeared from the surface up to 14 days' immersion. The degradation of MgCu coating could effectively kill *Staphylococcus aureus* with an antibacterial rate of 99% (Yu *et al.*, 2018).

Adding reactive elements to the surfaces of titanium alloys, such as Cu, Ce or elements like Si and F may increase the proliferation of osteoblasts while showing a decrease in bacteria (Santos-Coquillat *et al.*, 2018). Multifunctional coatings have been proposed to combine the wear-corrosion resistance, and to achieve proper amount osteoblast proliferation and bone matrix secretion while achieving a decrease in bacterial colonization.

However, the challenge of obtaining surfaces, which combine both good compatibility and an adequate degree of bactericide, has still not been achieved satisfactorily in the scientific literature.

In previous research works, the  $\text{TiO}_2/\text{CeO}_2$  coating on TiAlV has been evaluated as an alternative coating system for lengthening the useful life of TiAlV implants (Tavarez-Martínez *et al.*, 2019). Based on these good results and with the aim of furthering this research, in this work, heat treatment and posterior chemical conversion have been carried out on TiAlV surfaces to study if biocompatibility of the TiAlV can be improved and bacterial growth inhibited or reduced.

In our research, the cell line chosen has been mouse osteoblasts, responsible for the bone growth as they form a deposit of calcium and phosphorous (Patton and Thibodeau, 2007). The bacteria strain chosen was the *Staphylococcus epidermis* (Gram-positive) opportunistic pathogen cultured in aerobic conditions, due to several features: pathogenicity property, presence on the skin and mucus membranes, and ability to survive in high salt concentration media which contain 7-8% NaCl (Madigan *et al.*, 2003). *Staphylococcus epidermis* forms biofilms that grow on the devices, which are intro-

duced into the body like intravenous catheters and medical prostheses. The biofilm is the main virulence factor of this bacterium, acting as a barrier to antibiotics and host's immune response.

## 2. MATERIALS AND METHODS

### 2.1. Materials

The material under study was Ti6Al4V alloy with 19 mm in diameter and 3 mm thickness. The chemical composition by optical emission spectroscopy was (in wt.%): 88.9 Ti, 6.4 Al, 4.5 V and 0.2 Fe. The Ti6Al4V alloy was modified by thermal treatment (TiT hereafter) at 650 °C for 60 minutes, by means of a heating ramp (7 °C/min), into a furnace in oxygen rich atmosphere. After that, the piece was annealed at 450 °C (7 °C/min) for 15 minutes and then rapidly cooled in cold water.

After thermal treatment, half of the samples received a chemical conversion treatment consisting of immersion in a solution 0.001 M  $\text{CeCl}_3$  together with hydrogen peroxide ( $\text{H}_2\text{O}_2$ ) as oxidant for 15 minutes in order to obtain a surface layer of cerium oxide (called TiTCe throughout this paper).

All the modified samples were sonically cleaned in two steps: distilled water for three minutes followed by 96 % ethanol for five minutes. Finally, samples were dried in air and sterilized with ultra violet radiation for 60 minutes on each side.

### 2.2. Surface characterization by atomic force microscopy, AFM

The characterization of the surface modifications of Ti6Al4V was performed by means of an AFM 5100 (Agilent) equipped with a scanner with maximum ranges of 100  $\mu\text{m}$  in "x" and "y" scales and 4  $\mu\text{m}$  in "z" scale. The images were acquired in the tapping mode using a cantilever of silicon nitride, with a nominal probe curvature radius of 10 nm and a constant force of 40 N/m. The software WSxM (Nanotec) was used for processing the images.

### 2.3. Cell Culture

MC3T3-E1 cell line (from the cell bank of the Center for Biological Researches, CIB-CSIC, Madrid, Spain) was chosen as the mouse pre osteoblast cells.

The cells were incubated in 90 ml of Dulbecco's Modified Medium, (DMEM, Gibco®), 1ml of L-Glutamine 200 mM (Gibco®), 1 ml of Penicillin-Streptomycin (Gibco®), 1 ml of Sodium Pyruvate (Gibco®) and 10 ml of Fetal Bovine Serum (FBS, Sigma-Aldrich®) at 37 °C in a humidified atmosphere of 5%  $\text{CO}_2$  in air. The culture medium was changed every 2 or 3 days.

An initial concentration of 14000 cells/ml was seeded on 2.8 cm<sup>2</sup> of each experimental Ti6Al4V surface in the culture plate. Viability of the cell cultures was assessed by parallel control tests of osteoblasts on polystyrene culture plate. After 1, 3 and 7 days, cells were detached from the culture plate with trypsin-EDTA solution (Gibco-R) for 5 minutes in an incubator at 37 °C. Then, trypsin was neutralized by adding DMEM culture medium. Aliquots were loaded of 10 µl of cells suspended in DMEM on Neubauer camera and the cells were counted. Each experiment was carried out in triplicate.

Growth curves of MC3T3-E1 osteoblasts were obtained to compare the proliferation on the different modified Ti6Al4V surfaces.

#### 2.4. Cell fixation by SEM/EDX

Morphological and chemical studies of the osteoblast cells seeded on the modified Ti6Al4V surfaces after 1, 3 and 7 days were carried out. After each testing time the cells were fixed on the modified Ti6Al4V surfaces by adding 1 ml of 2% glutaraldehyde in phosphate buffer solution (PBS) at 4 °C for 24 hours. After that, cells were dehydrated at 4 °C for successively immersion in a series of ethanol solutions ranging from 35% to 100%. Tetramethylsilane solution (TMS Sigma-Aldrich®) at 50% (0.5 ml of TMS in 0.5 ml of 100 % ethanol) was added for 10 minutes to dry the surface-adhered cells. This solution was removed and 1 ml of TMS at 100% was added for another 10 minutes. Lastly, TMS was removed and left to air-dry during 30 minutes. Then, the osteoblasts adhered on the modified surfaces were topographically and chemically characterized by SEM and EDX (Hitachi S-4800) with a voltage of 5 kV and 15 kV, respectively.

#### 2.5. Biofilm formation

The biofilm formation was assessed with the strain *Staphylococcus epidermis* ATCC 35983 provided by American Type Collection Culture. The bacterial cultures were incubated in aerobic conditions for 18 h at 37 °C in Trypticase Soy Broth (TSB) (BBL, Becton Dickinson and Company, Sparks, USA). The bacterial suspensions were prepared in the exponential growth phase. The culture was adjusted up to a transmittance of 62% by means of horizontal light spectrophotometry (Helios Epsilon model, Thermo Spectronic, Thermo Fisher Scientific Inc., Cambridge UK), at a wavelength ( $\lambda$ ) of 492 nm. A bacterial inoculation of approximately 3x10<sup>8</sup> colony-forming unit (CFU)/ml at 37 °C with orbital movement (30 rpm) for 90 minutes to facilitate the adhesion was added to each surface. The samples were incubated for 24 hours at 37 °C and, the bacterial viability was quantified through its content in adenosine triphos-

phate (ATP) as a measure of metabolic activity. Then, they were transferred to new culture flasks and BacTiter-Glo™ Microbial Cell Viability Assay (Promega Corporation, Madison, WI, USA) was added for 10 minutes using an orbital movement in a dark chamber. Finally, the solution was transferred to white polystyrene microtiter plates in order to quantify its luminescence. The emission of light (the luciferin-luciferase reaction) was measured by a luminometer (Microplate Fluorescent Reader FLX 800, Biotek Instruments Inc). Each experiment was carried out in duplicate, in static flow, with orbital movement and was repeated two times for TiAlV, TiT and TiTCe samples in order to confirm the reproducibility of the different cultures. The surface area of the experimental sample was 2.8 cm<sup>2</sup>. The viability of the biofilm was represented as Relative Light Units, RLU%.

For the observation of the cells arrangement in the bacterial biofilm on the different surfaces, a scanning electron microscopy, SEM (Quanta 3D FEG FEI Company Hillsborough, US) with a detector electrons secondary detector, ETD, was used. The surfaces covered with bacterial biofilm were fixed with glutaraldehyde at 3% for 12-15 hours at room temperature. Immediately afterwards, the dehydration was carried out in successive concentrations of ethanol (from 30% to pure ethanol) for one hour in each one of them. Finally, the samples were metalized with an Au film of less than 5 nm thickness by cathodic spraying (Emitech K575X sputter coater).

#### 2.6. Statistical Analysis

All the quantitative studies were carried out in triplicate. The resulting data were statistically analyzed by a two-tailed student's t-test and expressed as a mean  $\pm$ SD. Differences were considered to be significant at  $p < 0.05$ . The correlation between different time interval studies was determined using Pearson's correlation coefficient.

### 3. RESULTS

Figure 1 shows the surface topography by AFM of TiAlV in as-reception (A), after thermal treatment (B) and subsequent treatment with Cerium chloride (C). In as-received condition, the lines proper to the surface preparation (grounding) can be seen (Fig. 1A). In the thermally treated sample (TiT) appear crystals of TiO<sub>2</sub> with rutile structure verified by DRX (Fig. 1B) (Tavaréz-Martínez *et al.*, 2019). The surfaces of the samples treated thermally and chemically (TiTCe) are more homogenous due to the cerium oxide deposited in pores and defects left by the thermal treatment. The thickness of the layer of cerium oxide is very thin as could be seen only by XPS (Tavaréz-Martínez *et al.*, 2019).

Table 1 reveals the RMS roughness parameter obtained from the different TiAlV samples by

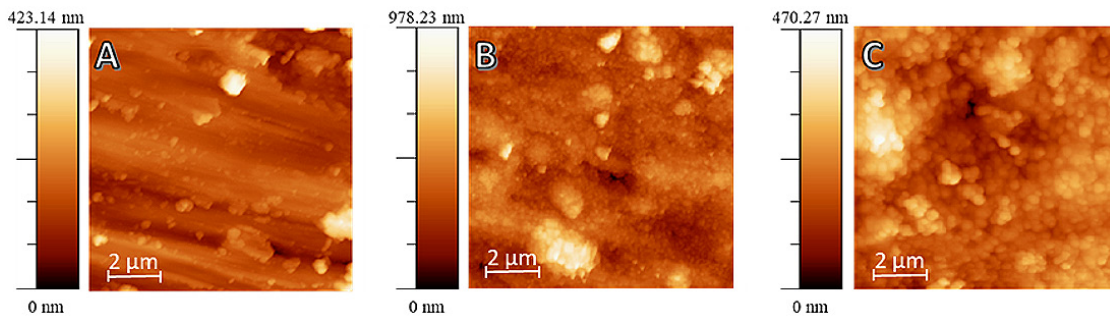


FIGURE 1. Topography by AFM of A) TiAlV, B) TiT and C) TiTce surfaces.

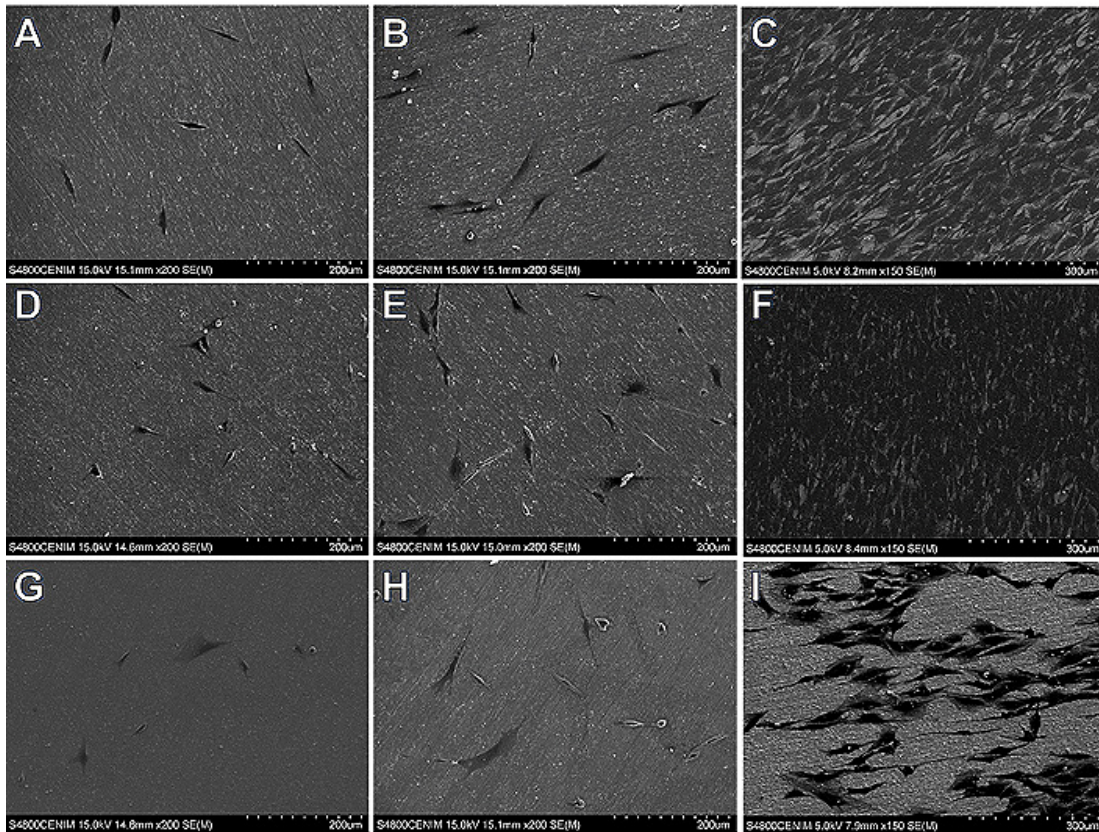


FIGURE 2. Secondary electron images of MC3T3-E1 osteoblasts after 1, 3 and 7 days on culture (A, B, C) TiAlV, (D, E, F) TiT and (G, H, I) TiTce surfaces, respectively.

TABLE 1. Average roughness measured by AFM

Sample	Area $\mu\text{m}^2$	RMS nm
TiAlV	10x10	99.3
	10x10	115.95
TiT	20x20	151.0
	50x50	166.2
TiTce	10x10	127.49
	20x20	150
	50x50	163

AFM. The roughness increases as a consequence of thermal treatment. The chemical treatment with cerium salts does not introduce any important changes in the roughness of the thermally treated samples.

Osteoblasts MC3T3-E1 cells were added on the different surfaces in order to compare the cell proliferation. Figure 2 shows the osteoblasts MC3T3-E1 cultivated after 1, 3, and 7 days in as-received Ti6Al4V (images A, B and C), thermally treated Ti6Al4V, TiT, (images D, E and F), and thermally and chemically treated TiAlV, TiTce, (images G, H and I), respectively.

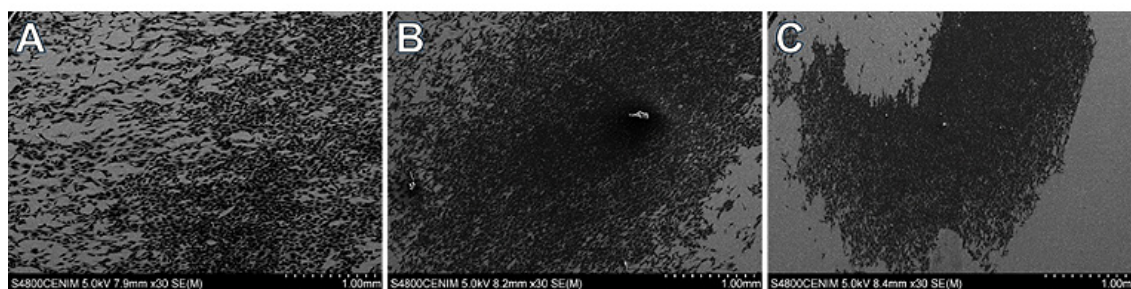


FIGURE 3. Secondary electron images of the MC3T3-E1 osteoblasts adhered on (A) TiAlV, (B) TiT and (C) TiTCe surfaces after 7 days in culture.

The elongated forms of the osteoblast cell with the extension of the filopodia to approach the other cells, are clearly shown. Good adhesion to the different surfaces is also observed. Figure 3 shows comparatively the two modified and as-received Ti6Al4V surfaces after seven days of culture. In general, the cell proliferation on samples TiTCe is adequate but the confluence is not achieved as occurs in both thermally treated and as-received Ti6Al4V surfaces.

The TiT showed the greatest amount of cell proliferation over testing time. The osteoblasts continued growing considerably on the TiT samples over testing time from the first day of culture, while the TiTCe surfaces showed the least cell proliferation. These data agree with that observed by SEM (Figs. 2 and 3). Although the cell proliferation is less in the TiTCe samples, the osteoblast cell morphology and adhesion to the Ce oxide layer (Fig. 2 photo I) revealed a good health and biocompatibility of the cells and so the absence of any cytotoxic effects. In summary, a good adhesion with an elongated morphology of the osteoblasts was observed on all the surfaces. Results are similar to that obtained by Cerro *et al.* (2002) with their experiments on porous hydroxyapatite.

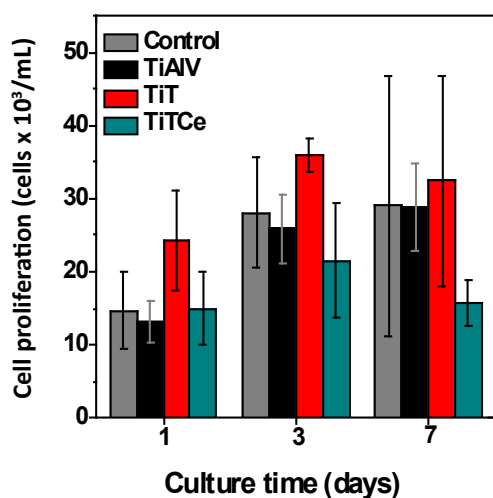


FIGURE 4. Cell proliferation of MC3T3-E1 osteoblasts on TiAlV, TiT and TiTCe.

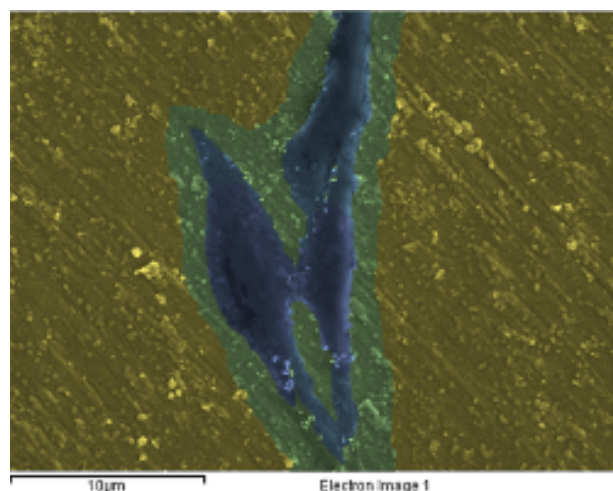


FIGURE 5. Secondary electron image of a MC3T3-E1 osteoblast on the Ti surface delimiting the three regions analyzed by EDX: sample surface (yellow), cells (dark blue) and extracellular matrix (green).

Figure 4 shows the cell proliferation of MC3T3-E1 osteoblasts on TiAlV, TiT and TiTCe. It can be seen that the highest proliferation is obtained for TiT surfaces. However, those TiTCe surfaces treated with Ce decrease considerably the proliferation.

A semi quantitative chemical analysis by EDS on the modified surfaces covered with cells for 1, 3 and 7 days was performed. Figure 5 shows the three regions analyzed: sample surface (yellow), cells (dark blue), and the area between cells filled with extracellular matrix, EM (green). Tables 2, 3 and 4 summarize the chemical analyses on these areas in the as-received Ti6Al4V, thermally treated TiT, and chemically treated TiTCe, respectively after 7 days in culture.

In as-received TiAlV, the surface is composed of Ti, Al and V in accordance with those obtained by optical emission spectroscopy, in wt. %: 6.4 Al, 4.5 V, 0.2 Fe and 88.9 Ti, corresponding to the ASTM F136 standard specification (Table 2). The C content is assigned to the handling of the samples. The chemical analysis on the cells (dark blue) reveals

TABLE 2. EDS analysis of TiAlV surfaces with MC3T3-E1 osteoblasts. (at.%)

	C	O	Ti	Al	V	Ce	Na	Cl	P	Ca	S
Surface	13.1	12.8	64.6	6.6	2.8				0.1	0.0	
Osteoblast	41.4	29.0	26.0	2.1	0.8				0.5	0.1	
Extracellular matrix	21.6	23.0	47.9	6.1	1.4						

TABLE 3. EDS analysis of TiT surfaces with MC3T3-E1 osteoblasts. (at.%)

	C	O	Ti	Al	V	Ce	Na	Cl	P	Ca	S
Surface	8.1	50.0	37.3	3.3	1.2				0.2		
Osteoblast	53.8	32.1	10.6	1.4	0.5		0.5	0.5	0.5	0.0	0.1
Extracellular matrix	21.7	51.4	22.7	2.8	1.3				0.1	0.0	0.0

TABLE 4. EDS analysis of TiTCe surfaces with MC3T3-E1 osteoblasts. (at.%)

	C	O	Ti	Al	V	Ce	Na	Cl	P	Ca	S
Surface	9.0	55.5	30.9	3.1	1.0	0.4			0.1	0.0	
Osteoblast	58.8	27.7	9.5	1.3	0.4	0.0	0.8	0.7	0.5	0.1	0.2
Extracellular matrix	32.0	43.8	19.8	1.6	0.9	0.1		0.2	0.1	0.0	

an increase in carbon, oxygen and phosphorous content with respect to the area without any cells (Table 2) and the presence of sulfur on the modified surfaces. These are the main constituents of the phospholipids, which form a high percentage of the biological membranes. In the area between the cells (green), the atomic percentages values of carbon, oxygen and phosphorus are between those of the metallic surface (yellow) and the cells (dark blue).

In the TiT samples, the atomic percentage of oxygen on the surface has increased substantially, (Table 3) due to the thermal treatment.

Finally, the chemically treated samples, TiTCe, appear covered with a thin layer of cerium (Table 4). These results are comparable to those obtained by Brunelli *et al.* (2005), and they have also corroborated in other research works by XPS (Tavarez-Martínez *et al.*, 2019). Besides the small percentage of Ce, the atomic percentage of the different elements is practically the same as those of the TiT samples. There is not any difference in the composition of the different areas analyzed with respect to the time. (See the supplementary material, showing the analyses of the different samples under study with MC3T3-E1 osteoblast for 1, 3 and 7 days).

The biocompatibility is generally improved with the new surface modifications of Ti6Al4V alloy, but also it is important to find out whether these modified surfaces show evidence of the inhibition of bacterial reproduction.

The viability of the biofilm of *Staphylococcus epidermidis* ATCC 35983 on the TiAlV, TiT and TiTCe

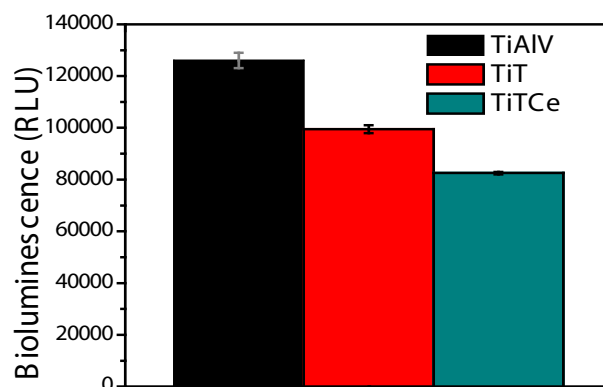


FIGURE 6. Bacterial viability of biofilm formed by *staphylococcus epidermidis* ATCC 35983 on TiAlV, TiT and TiTCe surfaces after 24 hours of incubation.

surfaces after 24 hours of growth is shown in Fig. 6. It can be observed that the thermal treatment decreases the bacterial viability and that this decrease is greater when they are coated with cerium oxide.

The Fig. 7 shows by scanning electron microscope the appearance of the biofilm architecture formed by the *Staphylococcus epidermis* ATCC 35983 strain after 24 hours of incubation on the surfaces.

It can be seen that there is a decrease in the bacterial growth on the treated surfaces with respect to the as-received TiAlV. SEM images only provide information about the bacteria adhered to the surface but cannot differentiate between metabolically active and dead bacteria. Nevertheless, a greater num-

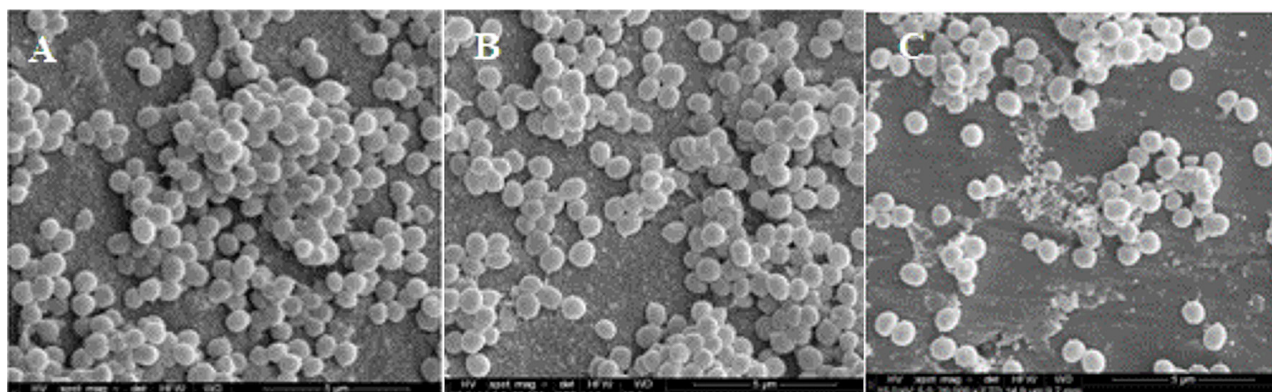


FIGURE 7. Electron micrographs (20000x) of the *Staphylococcus epidermidis* ATCC 35983 proliferation on (A) TiAlV, (B) TiT and (C) TiTCe surfaces after 24 hours of incubation.

ber of bacteria not so rounded, apparently damaged on the TiTCe surfaces in comparison to the as-received Ti6Al4V surface can be seen. Some of these bacteria are marked with arrowheads as an example.

#### 4. DISCUSSION

The process of the integration of the implant with the biological tissue, according to Kasemo and Lausmaa (1998) and Fathi *et al.* (2003), begins with the adsorption of the first water molecules on the surface of the implanted material. These molecules may interact in different ways. If the surface is hydrophilic, the water molecules adhere very strongly but if the surface is hydrophobic so water adheres weakly to the surface. Once the water molecules have interacted with the surface, the ions present in the biological medium, such as  $\text{Na}^+$  and  $\text{Cl}^-$  among others, are incorporated forming an electrochemical double layer.

In the case of the modified titanium surfaces tested in this work, the sodium and chloride ions were only seen on the TiT and TiTCe samples (Tables 2, 3, 4). According to Patton and Thibodeau (2007), these ions dissolved in water contribute to the fluidity of the extracellular matrix.

Subsequently, the proteins and other molecules approach the surface where they are adsorbed creating a layer of a mixture of different proteins in distinct states of conformation. Then, the cells which create interactions with the protein layer by means of the cellular extensions approach the cell membrane and the cell receptors. So, the response of the implanted material-cells depends largely on the type of proteins and their conformation. The result of this interaction may be the integration of the implant or rather the encapsulation of the implant in a fibrous layer or even its rejection.

In our experiments, the atomic percentage of carbon, oxygen and sulfur increased as a consequence of cells growth on materials studied. The sulfur especially increased in the presence of the  $\text{CeO}_2$  on the

thermally treated surface (Table 4). Shivakumar *et al.* analyzed the effect of cerium atoms on the synthesis of collagen in cultured cardiac fibroblasts and explants. It was shown that low concentrations of cerium (100 nM) enhanced the synthesis of collagen and high concentrations (100  $\mu\text{M}$ ) inhibited it (Fathi *et al.*, 2003).

In the spaces between the cells, i.e. the extracellular matrix, there is also an increase in carbon and oxygen in comparison with what occurs in the metallic matrix (Tables 2, 3, 4). Proteins are another important component which form the extracellular matrix and whose principal composition is carbon, oxygen and hydrogen (Patton and Thibodeau, 2007). The proteins may be structural fibers, glycoproteins or proteoglycans. The structural fibers like collagen and elastin give flexibility to the tissues (Bueno-Vera *et al.*, 2015). The glycoproteins are protein molecules attached to carbohydrates, among them, the integrins facilitate the adhesion between the cells and the extracellular matrix. The proteoglycans, like chondroitin sulphate, are hybrid molecules, which are made up principally of carbohydrates attached to the skeletons of proteins. In addition, some molecules contain sulfur, iron and phosphorous (Tables 2, 3, 4).

There are several factors that can affect the implant-cell interaction and may inhibit cell growth such as: the ion release and the chemical composition and topography of the surface under study. TiAlV is a material that is capable of passivating instantly with the oxygen in the air, forming a compact, uniform and adherent nano layer of  $\text{TiO}_2$ , which isolates metallic substrate and reducing considerably the ion release kinetics in very different corrosive media. The chemical composition of the as-received TiAlV alloy favors the formation of a passive layer of  $\text{TiO}_2$  of nanometer order. The heat treated alloy has a thicker layer (1  $\mu\text{m}$ ) of  $\text{TiO}_2$  of rutile while the TiTCe sample has also a thin layer of cerium oxide, in which the Ce is found in two possible  $\text{Ce}^{3+}/\text{Ce}^{4+}$  oxidation states (Tavaréz-Martínez *et al.*, 2019). The surface chemical composition of

the modified Ti substrates is important for the adsorption of proteins. In the case of the TiT samples, TiO<sub>2</sub> is highly hydrophilic, thus favoring the first step towards the metallic material/cell integration (Shivakumar *et al.*, 1992). In aqueous media, the OH<sup>-</sup> favors the bond with phosphate ions by means of the Ca<sup>2+</sup> ions (acting as a bridge) present in the physiological medium. The presence of ions like phosphate or calcium in the culture medium results in a positive stimulus for cell viability and therefore for the process of osseointegration of the implant in the organism. These ions appear in the different table (Tables 2, 3, 4) and some are deposits of calcium and phosphorous which can give rise to the formation of hydroxyapatite, providing the bone with mineralization and strength (Bueno-Vera *et al.*, 2015). These points serve to anchor the osteoblasts (Burgos Asperilla, 2013) (Fig. 2).

Most of the heat treatments applied to the TiAlV alloy are carried out in order to obtain a good adherent rutile-based surface with the aim of improving wear, corrosion resistance and biocompatibility. The rutile phase obtained is thermodynamically stable and according to several authors is more inert to a bacterial attack and has greater friction resistance compared to anatase and brockite (Izman *et al.*, 2012). Other studies have shown that the Young modulus of rutile structure is close to that of bone (Ayu *et al.*, 2017). Despite these encouraging properties, few research works have been reported on the adhesion strength of the oxide layer formed on the titanium substrate.

The smallest cell growth was obtained on the surface of TiTCe samples that is affected by the low affinity of cerium for water (Azimi *et al.*, 2013; Tavares Martínez, 2019), which is important in the implant-biological tissue interaction process. This hydrophobic character is due to the electronic structure of the oxides of the rare earths where 4f orbitals (not fully occupied), are protected from the interactions with the surrounding environment by the complete octet of electrons in the external layers 5s<sup>2</sup>p<sup>6</sup>. Therefore, they have less interaction with water molecules in the interface (Azimi *et al.*, 2013). However, it has been reported that by adding cerium oxide on boride surfaces (in the same way we obtained cerium oxide on TiO<sub>2</sub>), more uniform, smooth and crack free layers can be obtained, which increase the tribological performance as well as corrosion resistance of the TiAlV (Peng *et al.*, 2018; Tavares-Martínez *et al.*, 2019). The hydrophobic character of the compounds of Ce on the surfaces is not at all unfavorable, since the soluble compounds of Ce<sup>4+</sup> are associated mainly with a high redox potential of tetravalent cerium ions and the ability to oxidize biological molecules that can cause problems of toxicity. In addition, the Ce<sup>3+</sup> ions released from the layer at high concentrations may cause a Fen-

ton-like reaction in the biological medium. On the other hand, the nano ceria and cerium ions used in regenerative medicine have shown some interesting properties, as for example, stimulating the growth of fibroblasts and thereby helping the regeneration of the surrounding tissues (Shcherbakov *et al.*, 2020).

Other important parameter for cell adhesion and proliferation is the increase in surface roughness of the materials (Anselme and Bigerelle, 2005; Ahmed *et al.*, 2012). It has been noted that higher values of surface roughness provide better cell adhesion. It could be seen in Table 1 that the heat treatment increases the surface roughness but the subsequent chemical treatment with cerium salts does not introduce any significant changes in roughness. Accordingly, a greater cell proliferation has been obtained in the samples TiT (Figs. 2, 3 and 4).

In the experiments with bacteria on the modified Ti alloys, the smallest bacterial viability was shown by the surface treated with cerium salts, TiTCe, followed by that treated thermally and after by the as-received state (Fig. 6). The smallest proliferation occurring in the presence of the cerium oxide layer, concurred with other studies carried out by other authors (Pelletier *et al.*, 2010; Ciobanu and Harja, 2019; Shcherbakov *et al.*, 2020) where it was shown that the presence of nanocrystals of CeO<sub>2</sub> can inhibit the growth of some bacteria. This effect was explained on the basis of different mechanisms, such as membrane disruption, ROS generation and interference with the nutrient transport functions (Alpaslan *et al.*, 2017). The electron micrographs of the biofilm formation on surfaces (Fig. 7) showed a higher number of not turgid bacteria in the TiTCe surface, possibly due to membrane damage.

Cerium oxide nanoparticles possess anti-inflammatory properties. Nanoceria reduces the production of inflammatory mediators by stimulating the macrophages of mice cell line J774A. In a model of human immunity in vitro, Schanen *et al.* (2013) found that the treatment with CeO<sub>2</sub> nanoparticles induced APCs (antigen-presenting cells) to secrete the anti-inflammatory cytokine, IL-10 and a TH2-dominated T cell profile (Shcherbakov *et al.*, 2020).

Nevertheless, according to our research, it is too early to state that cerium oxide has a bactericidal effect. Some factors have to be taken into account such as, the morphology of the nanoceria, the pH of the medium, the nature of the bacteria itself (differences on the surface of the membrane, metabolic differences and/or potential effects on the formation of spores) and, especially, the Ce<sup>3+</sup>/Ce<sup>4+</sup> ratio. An elevated quantity of Ce<sup>3+</sup> cause an antioxidant effect. Otherwise, if Ce<sup>3+</sup>/Ce<sup>4+</sup> ratio is low, act as an anticarcinogenic and antibacterial agent (Alpaslan *et al.*, 2017).

However, the decrease in bacterial viability, observed in this work, is a good progress, since the in-

crease in hydrophobicity and roughness is normally associated with an increase in bacterial adhesion to surfaces (Donlan, 2002; Boyd *et al.*, 2002).

## 5. CONCLUSIONS

- The TiAlV treated thermally showed greater osteoblast proliferation because of its coating of rutile and higher roughness values compared to the other tested TiAlV surfaces.

- The TiAlV surfaces after thermal and, specially, chemical treatment with cerium oxide showed a decrease in the bacterial adhesion of *Staphylococcus epidermis*.

## ACKNOWLEDGMENTS

The authors all declare that they have not conflict of interest.

The authors thank María Carabajo-Sánchez for the technical assistance with SEM for the biofilm Images, in the “Servicio de análisis y caracterización de sólidos y superficies (SACSS)” within the University of Extremadura (Spain).

Funding: This work was supported by CONACYT [Basic science project 2012 #183416, SIP Project 20160107]; Ministerio de Economía y Competitividad [MAT2015-63974-C4-4-R.]; Ministerio de Ciencia e Innovación [RTI2018-101506-B-C31]; and Junta de Extremadura-FEDER [GR18096].

ANNEXES: Supplementary material is attached.

## REFERENCES

- Ahmed, M.H., Byrne, J.A., Keyes, T.E., Ahmed, W., Elhissi, A., Jackson, J., Ahmed, E. (2012). *Characteristics and applications of titanium oxide as a biomaterial for medical implants. in The Design and Manufacture of Medical Devices*. Woodhead Publishing, Oxford Cambridge Philadelphia New Delhi, pp. 1–57. <https://doi.org/10.1533/9781908818188.1>.
- Alpaslan, E., Geilich, B.M., Yazici, H., Webster, T.J. (2017). pH-Controlled Cerium Oxide Nanoparticle Inhibition of Both Gram-Positive and Gram-Negative Bacteria Growth. *Sci. Rep.* 7, 45859. <https://doi.org/10.1038/srep45859>.
- Anselme, K., Bigerelle, M. (2005). Topography effects of pure titanium substrates on human osteoblast long-term adhesion. *Acta Biomater.* 1 (2), 211–222. <https://doi.org/10.1016/j.actbio.2004.11.009>.
- Ayu, H.M., Izman, S., Daud, R., Krishnamurthy, G., Shah, A., Tomadi, S.H., Salwani, M.S. (2017). Surface Modification on CoCrMo Alloy to Improve the Adhesion Strength of Hydroxyapatite Coating. *Procedia Eng.* 184 399–408. <https://doi.org/10.1016/j.proeng.2017.04.110>.
- Azimi, G., Dhiman, R., Kwon, H.-M., Paxson, A.T., Varanasi, K.K. (2013). Hydrophobicity of rare-earth oxide ceramics. *Nat. Mater.* 12, 315–320. <https://doi.org/10.1038/nmat3545>.
- Bauer, S., Schmuki, P., von der Mark, K., Park, J. (2013). Engineering biocompatible implant surfaces: Part I: Materials and surfaces. *Prog. Mater. Sci.* 58 (3), 261–326. <https://doi.org/10.1016/j.pmatsci.2012.09.001>.
- Boyd, R.D., Verran, J., Jones, M.V., Bhakoo, M. (2002). Use of the Atomic Force Microscope to determine the effect of substratum surface topography on bacterial adhesion. *Langmuir* 18 (6), 2343–2346. <https://doi.org/10.1021/la011142p>.
- Bral, A., Mommaerts, M.Y. (2016). In vivo biofunctionalization of titanium patient-specific implants with nano hydroxyapatite and other nano calcium phosphate coatings: A systematic review. *J. Cranio-Maxillofacial Surg.* 44 (4), 400–412. <https://doi.org/10.1016/j.jcms.2015.12.004>.
- Brunelli, K., Dabalà, M., Calliari, I., Magrini, M. (2005). Effect of HCl pre-treatment on corrosion resistance of cerium-based conversion coatings on magnesium and magnesium alloys. *Corros. Sci.* 47 (4), 989–1000. <https://doi.org/10.1016/j.corsci.2004.06.016>.
- Bueno-Vera, J.A., Torres-Zapata, I., Sundaram, P.A., Diffoot-Carlo, N., Vega-Olivencia, C.A. (2015). Electrochemical characterization of MC3T3-E1 cells cultured on  $\gamma$ TiAl and Ti–6Al–4V alloys. *Bioelectrochemistry* 106 (Par B), 316–327. <https://doi.org/10.1016/j.bioelectrochem.2015.06.012>.
- Burgos Asperilla, L. (2013). Caracterización y estudio electroquímico de superficies de Ti inmersas en medio fisiológico y en cultivo celular. Tesis PhD, Universidad Autónoma de Madrid.
- Cerroni, L., Filocamo, R., Fabbri, M., Piconi, C., Caropreso, S., Condò, S.G. (2002). Growth of osteoblast-like cells on porous hydroxyapatite ceramics: an in vitro study. *Biomol. Eng.* 19 (2-6), 119–124. [https://doi.org/10.1016/S1389-0344\(02\)00027-8](https://doi.org/10.1016/S1389-0344(02)00027-8).
- Ciobanu G., Harja, M. (2019). Cerium-doped hydroxyapatite/collagen coatings on titanium for bone implants. *Ceram. Int.* 45 (2), 2852–2857. <https://doi.org/10.1016/j.ceramint.2018.07.290>.
- Díaz-Gómez, L., Concheiro, A., Álvarez-Lorenzo, C. (2018). Functionalization of titanium implants with phase-transited lysozyme for gentle immobilization of antimicrobial lysozyme. *Appl. Surf. Sci.* 452, 32–42. <https://doi.org/10.1016/j.apsusc.2018.05.024>.
- Donlan, R.M. (2002). Biofilms: microbial life on surfaces. *Emerg. Infect. Dis.* 8 (9), 881–890. <https://doi.org/10.3201/eid0809.020063>.
- Fathi, M.H., Salehi, M., Saatchi, A., Mortazavi, V., Moosavi, S.B. (2003). In vitro corrosion behavior of bioceramic, metallic, and bioceramic-metallic coated stainless steel dental implants. *Dent. Mater.* 19 (3), 188–198. [https://doi.org/10.1016/S0109-5641\(02\)00029-5](https://doi.org/10.1016/S0109-5641(02)00029-5).
- Geetha, M., Singh, A.K., Asokamani, R., Gogia, A.K. (2009). Ti based biomaterials, the ultimate choice for orthopaedic implants – A review. *Prog. Mater. Sci.* 54, 397–425. <https://doi.org/10.1016/j.pmatsci.2008.06.004>.
- Germán-Salló, Z., Strnad, G. (2018). Signal processing methods in fault detection in manufacturing systems. *Procedia Manuf.* 22, 613–620. <https://doi.org/10.1016/j.promfg.2018.03.089>.
- Hernández-López, J.M., Conde, A., de Damborenea, J.J., Arenas, M.A. (2016). Electrochemical response of TiO<sub>2</sub> anodic layers fabricated on Ti6Al4V alloy with nanoporous, dual and nanotubular morphology. *Corros. Sci.* 112, 194–203. <https://doi.org/10.1016/j.corsci.2016.07.021>.
- Izman, S., Abdul-Kadir, M.R., Anwar, M., Nazim, E.M., Rosliza, R., Shah, A., Hassan, M.A., (2012). *Surface Modification Techniques for Biomedical Grade of Titanium Alloys: Oxidation, Carburization and Ion Implantation Processes*. In *Titanium Alloys*. Chapter 9, IntechOpen, Rijeka. <https://doi.org/10.5772/36318>.
- Jackson, M.J., Ahmed W. (2007). *Titanium and Titanium Alloy Applications in Medicine. In Surface Engineered Surgical Tools and Medical Devices*. Springer US, Boston, pp. 533–576. [https://doi.org/10.1007/978-0-387-27028-9\\_15](https://doi.org/10.1007/978-0-387-27028-9_15).
- Jenko, M., Gorenšek, M., Godec, M., Hodnik, M., Batič, B.Š., Donik, Č.J., Grant, T., Dolinar, D. (2018). Surface chemistry and microstructure of metallic biomaterials for hip and knee endoprostheses. *Appl. Surf. Sci.* 427, 584–593. <https://doi.org/10.1016/j.apsusc.2017.08.007>.
- Kasemo, B., Lausmaa, J. (1988). Biomaterial and implant surfaces: a surface science approach. *Int. J. Oral Maxillofac. Implants* 3 (4), 247–259.
- Madigan, M.T., Martinko, J.M., Parker, J. (2003). *Brock. Biología de los microorganismos*. 10th ed., Pearson Educación, Madrid.

- Mareci, D., Lucero, V., Mirza, J. (2009). Effect of replacement of vanadium by iron on the electrochemical behaviour of titanium alloys in simulated physiological media. *Rev. Metal.* 45 (1), 32–41. <https://doi.org/10.3989/revmetalm.0750>.
- Niinomi, M. (2002). Recent metallic materials for biomedical applications. *Metall. Mater. Trans. A* 33, 477. <https://doi.org/10.1007/s11661-002-0109-2>.
- Patton, K.T., Thibodeau, G.A. (2007). *Anatomía y Fisiología*. 6th ed., Elsevier, Barcelona.
- Pelletier, D.A., Suresh, A.K., Holton, G.A., McKeown, C.K., Wang, W., Gu, B., Mortensen, N.P., Allison, D.P., Joy, D.C., Allison, M.R., Brown, S.D., Phelps, T.J., Doktycz, M.J. (2010). Effects of Engineered Cerium Oxide Nanoparticles on Bacterial Growth and Viability. *Appl. Environ. Microbiol.* 76 (24), 7981–7989. <https://doi.org/10.1128/AEM.00650-10>.
- Peng, M.J., Duan, Y.H., Ma, L.S., Shu, B.P. (2018). Characteristics of surface layers on Ti6Al4V alloy borided with CeO<sub>2</sub> near the transition temperature. *J. Alloys Compd.* 769, 1–9. <https://doi.org/10.1016/J.JALLCOM.2018.07.365>.
- Raphel, J., Holodniy, M., Goodman, S.B., Heilshorn, S.C. (2016). Multifunctional coatings to simultaneously promote osseointegration and prevent infection of orthopaedic implants. *Biomaterials* 84, 301–314. <https://doi.org/10.1016/j.biomaterials.2016.01.016>.
- Santander, S., Alcaine, C., Lyahyi, J., Pérez, M.A., Rodellar, C., Doblaré, M., Ochoa, I. (2014). *In vitro* osteoinduction of human mesenchymal stem cells in biomimetic surface modified titanium alloy implants. *Dent. Mater. J.* 33 (3), 305–312. <https://doi.org/10.4012/dmj.2012-015-r>.
- Santos-Coquillat, A., Gonzalez Tenorio, R., Mohedano, M., Martinez-Campos, E., Arrabal, R., Matykina, E. (2018). Tailoring of antibacterial and osteogenic properties of Ti6Al4V by plasma electrolytic oxidation. *Appl. Surf. Sci.* 454, 157–172. <https://doi.org/10.1016/j.apsusc.2018.04.267>.
- Schanen, B.C., Das, S., Reilly, C.M., Warren, W.L., Self, W.T., Seal, S., Drake, D.R. (2013). Immunomodulation and T Helper TH1/TH2 Response Polarization by CeO<sub>2</sub> and TiO<sub>2</sub> Nanoparticles. *PLOS ONE* 8, e62816. <https://doi.org/10.1371/journal.pone.0062816>.
- Shcherbakov, A.B., Zholobak, N.M., Ivanov, V.K. (2020). *Biological, biomedical and pharmaceutical applications of cerium oxide. In Metal Oxides Series Cerium oxide (CeO<sub>2</sub>): Synthesis, Properties and Applications*. Elsevier, Amsterdam, 279–358. <https://doi.org/10.1016/B978-0-12-815661-2.00008-6>.
- Shivakumar, K., Nair, R.R., Valiathan, M.S. (1992). Paradoxical effect of cerium on collagen synthesis in cardiac fibroblasts. *J. Mol. Cell. Cardiol.* 24 (7), 775–780. [https://doi.org/10.1016/0022-2828\(92\)93391-V](https://doi.org/10.1016/0022-2828(92)93391-V).
- Simsek, I., Ozyurek, D. (2019). Investigation of the wear and corrosion behaviors of Ti5Al2.5Fe and Ti6Al4V alloys produced by mechanical alloying method in simulated body fluid environment. *Mater. Sci. Eng. C* 94, 357–363. <https://doi.org/10.1016/j.msec.2018.09.047>.
- Siqueira, R.P., Sandim, H.R.Z., Hayama, A.O.F., Henriques, V.A.R. (2009). Microstructural evolution during sintering of the blended elemental Ti–5Al–2.5Fe alloy. *J. Alloys Compd.* 476 (1–2), 130–137. <https://doi.org/10.1016/j.jallcom.2008.09.004>.
- Sittig, C., Textor, M., Spencer, N.D., Wieland, M., Vallotton, P.H. (1999). Surface characterization. *J. Mater. Sci. Mater. Med.* 10, 35–46. <https://doi.org/10.1023/A:1008840026907>.
- Srivivas, P.K., Kapat, K., Das, B., Pal, P., Ray, P.G., Dhara, S. (2019). Hierarchical surface morphology on Ti6Al4V via patterning and hydrothermal treatment towards improving cellular response. *Appl. Surf. Sci.* 478, 806–817. <https://doi.org/10.1016/j.apsusc.2019.02.039>.
- Tavarez Martínez, G. de M. (2019). Evaluación de recubrimientos TiO<sub>2</sub>-CeO<sub>2</sub> sobre la aleación Ti6Al4V, mediante técnicas electroquímicas convencionales y de campo próximo en presencia de células vivas. Tesis (Maestría en Tecnología Avanzada), Instituto Politécnico Nacional. <http://tesis.ipn.mx/handle/123456789/26595>.
- Tavarez-Martínez, G.M., Onofre-Bustamante, E., De La Cruz-Terrazas, E.C., Escudero-Rincón, M.L., Domínguez-Crespo, M.A. (2019). Evaluation of TiO<sub>2</sub>/CeO<sub>2</sub> coating on Ti6Al4V alloy in PBS physiological medium using conventional and near field electrochemical techniques. *Appl. Surf. Sci.* 494, 1109–1118. <https://doi.org/10.1016/j.apsusc.2019.07.066>.
- Weng, Y., Liu, H., Ji, S., Huang, Q., Wu, H., Li, Z., Wu, Z., Wang, H., Tong, L., Fu, R.K.Y., Chu, P.K., Pan, F. (2018). A promising orthopedic implant material with enhanced osteogenic and antibacterial activity: Al<sub>2</sub>O<sub>3</sub>-coated aluminum alloy. *Appl. Surf. Sci.* 457, 1025–1034. <https://doi.org/10.1016/j.apsusc.2018.06.233>.
- Wu, S., Liu, X., Yeung, K.W.K., Liu, C., Yang, X. (2014). Biomimetic porous scaffolds for bone tissue engineering. *Mater. Sci. Eng. R Reports* 80, 1–36. <https://doi.org/10.1016/j.mser.2014.04.001>.
- Yang, D.H., Moon, S.W., Lee, D.-W. (2017). Surface Modification of Titanium with BMP-2/GDF-5 by a Heparin Linker and Its Efficacy as a Dental Implant. *Int. J. Mol. Sci.* 18 (1), 229. <https://doi.org/10.3390/ijms18010229>.
- Yu, X., Ibrahim, M., Lu, S., Yang, H., Tan, L., Yang, K. (2018). MgCu coating on Ti6Al4V alloy for orthopedic application. *Mater. Lett.* 233, 35–38. <https://doi.org/10.1016/j.matlet.2018.08.063>.
- Zorn, G., Baio, J.E., Weidner, T., Migonney, V., Castner, D.G. (2011). Characterization of Poly(sodium styrene sulfonate). Thin Films Grafted from Functionalized Titanium Surfaces. *Langmuir* 27, 13104–13112. <https://doi.org/10.1021/la201918y>.

**ANNEXES. SUPPLEMENTARY MATERIAL**

EDS analysis of TiAlV samples with MC3T3-E1 osteoblasts at different times. (at.%)

day	Surface sample			Osteoblast			Extracellular matrix		
	1	3	7	1	3	7	1	3	7
C	44.9	13.8	27.8	58.3	48.9	29.6	54.7	27.2	12.1
O	5.0	62.8	24.8	28.0	37.0	27.3	22.9	22.4	14.4
Ti	41.4	19.1	40.9	10.7	7.9	36.5	18.2	41.2	63.5
Al	7.4	3.5	4.1	1.7	1.6	4.8	3.1	7.9	7.2
V	1.3	0.8	2.4	0.4	0.4	1.6	0.6	1.0	2.8
Ce	-	-	-	-	-	-	-	-	-
Na	-	-	-	0.3	0.5	0.1	0.1	-	-
Cl	-	-	-	0.3	0.5		0.2	0.1	-
P	-	-	-	0.2	0.2	0.1	0.1	0.1	-
Ca	-	-	-	-	2.9	-	-	-	-
S	-	-	-	-	0.2	-	-	-	-

EDS analysis of TiT samples with MC3T3-E1 osteoblasts at different times. (at.%)

day	Surface sample			Osteoblast			Extracellular matrix		
	1	3	7	1	3	7	1	3	7
C	17.5	15.8	7.8	66.4	68.3	53.4	18.8	14.4	10.4
O	62.1	65.5	-	25.7	20.8	31.0	59.6	67.1	59.9
Ti	16.4	14.9	83.5	1.6	2.5	11.5	17.9	15.2	25.5
Al	3.2	3.0	5.4	0.5	0.8	1.6	3.0	2.7	2.6
V	0.5	0.5	3.3	0.1	0.1	0.4	0.5	0.3	1.3
Ce	-	-	-	-	-	-	-	-	-
Na	0.1	0.2	-	3.0	4.1	0.8	0.2	0.1	-
Cl	-	-	-	2.3	3.0	0.7	-	0.1	0.2
P	-	-	-	0.4	0.3	0.3	-	0.1	-
Ca	-	-	-	-	-	-	-	-	-
S	-	-	-	-	0.1	0.2	-	-	-

EDS analysis of TiTCe samples with MC3T3-E1 osteoblasts at different times. (at.%)

day	Surface sample			Osteoblast			Extracellular matrix		
	1	3	7	1	3	7	1	3	7
C	9.5	13.4	16.5	67.9	66.9	53.8	17.4	41.2	23.0
O	64.7	66.9	49.8	29.1	24.2	31.9	63.1	46.9	51.5
Ti	21.8	15.6	28.9	0.2	3.0	10.9	16.1	7.8	21.6
Al	2.9	2.7	3.0	0.1	0.7	1.2	2.6	2.1	2.3
V	0.7	0.5	1.0	-	0.1	0.4	0.4	0.6	0.7
Ce	-	0.1	0.1	-	-	-	0.1	0.1	-
Na	0.1	0.5	0.4	1.0	2.6	0.8	0.1	0.8	0.3
Cl	0.1	0.2	0.2	1.1	1.9	-	-	0.4	0.3
P	0.1	0.1	0.1	0.3	0.3	0.1	0.1	0.1	0.1
Ca	-	-	-	-	-	0.7	-	-	-
S	-	-	-	0.2	0.1	0.2	-	-	0.1